

CHITOSAN/SILK FIBROIN/ZINC OXIDE NANOCOMPOSITE AS A SUSTAINABLE AND ANTIMICROBIAL BIOMATERIAL

AHMED SALAMA

*Cellulose and Paper Department, National Research Centre, 33, El-Bohouth Str.,
Dokki, P.O. 12622, Giza, Egypt*

✉ *Corresponding author: ahmed_nigm78@yahoo.com*

Received March 5, 2017

In the current study, a chitosan/silk fibroin blend was developed as a sustainable, cost-effective and bioactive material for embedding zinc oxide nanoparticles. Zinc oxide nanoparticles with the diameter less than 10 nm and uniform size distribution were examined with different characterization tools. The chitosan/silk fibroin/zinc oxide nanocomposite exhibited the advantage of broad antibacterial activities against bacteria. The hydrophilicity and swellability were significantly improved after the blending of chitosan and zinc oxide. The results exhibited that the chitosan/silk fibroin/zinc oxide, a disinfection nanocomposite for effective inhibition of bacterial growth, holds great promise for biomedical applications, especially in wound dressing.

Keywords: chitosan, silk, zinc oxide, nanocomposite, antibacterial material

INTRODUCTION

Zinc oxide nanoparticles have received considerable interest as a promising material due to their non-toxicity, cost-effectiveness and high adsorption capacity.¹ Moreover, these particles were recently applied in many applications, such as catalysis,² biomedical applications,³ textiles, cosmetics and food additives.⁴ In addition, zinc oxide nanoparticles are reported as a safe material with broad antibacterial activities.^{5,6} Due to their unique properties, zinc oxide nanoparticles have been utilized as reinforcing filler in polymer composites. The major challenge here is to mineralize small-sized zinc oxide nanoparticles with uniform size distribution, orientation and shape.

Natural polymers have relatively rarely been studied in the context of inorganic mineralization. During the last few years, our research group has made significant progress in studying the effects of natural polymers, especially polysaccharides, for the biomimetic growth of calcium phosphate.^{7,8} Moreover, these studies present new polysaccharide/calcium phosphate hybrid materials as a candidate for bone tissue engineering.

Organic matrix mediated biomineralization systems, such as collagen, amino acids and

polyelectrolytes, have been found to play an important role as templates for controlling inorganic nanoparticles like hydroxyapatite in living organisms.⁹ Inspired by biomineralization, polymers with charged functional groups have been used for inducing nucleation of inorganics, such as calcium phosphate,^{10,11} calcium carbonate¹² and titanium oxides.¹³ Chitosan has been studied in different biomedical applications due to its ready availability, biocompatibility and osteoconductivity.^{14,15} Although neat chitosan has many properties required for tissue engineering scaffolds, it is too brittle in aqueous solution to be used in cyclical loading applications. Several techniques have been used to overcome the drawbacks of chitosan in biomedical applications.¹⁶⁻¹⁸ Among them, blending with bioactive and functionalized polymers has been reported as a strategy for improving its physical properties.

Silk fibroin, extracted and purified from silkworm (*Bombyx mori*) cocoons,¹⁹ has recently gained increasing interest as a biomaterial due to its biocompatibility, relatively slow degradation *in vivo*, excellent mechanical performance and its ability to induce minimal immune and inflammatory responses when implanted in the

body.²⁰ Silk fibroin is composed of 17 amino acids and has been recently utilized in bone regeneration,²¹ wound dressing²² and drug delivery.²³ In the field of inorganic mineralization, hierarchically porous silk fibroin octacalcium phosphate showed greatly enhanced cellular responses with considerable potential for hard tissue applications.²⁰ Lijie Liu *et al.*²⁴ investigated calcium carbonate mineralization in the presence of silk fibroin. The resulting monodisperse vaterite microspheres have good encapsulation efficiency and pH sensitivity as drug carriers for doxorubicin.

The present study describes the use of a completely green material prepared from chitosan/silk fibroin as a bioactive blend for zinc oxide mineralization. The developed chitosan/silk fibroin/zinc oxide nanocomposite is expected to find promising applications in wound healing.

EXPERIMENTAL

Materials

Chitosan, with a molecular weight from 190,000 to 370,000 Da and degree of deacetylation not less than 75%, was purchased from Sigma-Aldrich. Lithium bromide and zinc acetate dehydrate were also obtained from Sigma-Aldrich. All the reagents were of analytical grade and used as received without further purification.

Preparation of regenerated chitosan/silk fibroin blend and zinc oxide precipitation

Bombyx mori cocoons were purified from their sericin content, using the method reported by Qi *et al.*²⁵ Briefly, sericin protein was removed by boiling the silkworm cocoons for 40 min in an aqueous solution of 0.5% (w/v) Na₂CO₃ and then rinsing them thoroughly with boiled distilled water. The purified silk fibers were dissolved in 9.3 mol/L LiBr solution at 60 °C for 1 h. The solution was dialyzed in deionized water at room temperature for 3 days to remove LiBr. The final concentration of the silk fibroin was 6.0% (w/v), which was determined by drying a known volume and weighing. The dialyzed silk fibroin aqueous solution was collected and stored at 4 °C until further use. After preparing a 2% chitosan solution in 2% acetic acid, the chitosan/silk fibroin blend was prepared by mixing the chitosan and silk fibroin solutions in a 50:50 ratio (wt:wt) under continuous stirring for 6 hours. The chitosan/silk fibroin blend was coagulated by pouring excess ethanol until complete precipitation. Then, the coagulated chitosan/silk fibroin was subjected to filtration and freeze drying. The regenerated chitosan/silk fibroin blend was immersed in a 2% zinc acetate solution, followed by adding 0.1 M sodium hydroxide solution until it reached pH 7.

The mixture was kept under stirring for 1 hour and then the blend was removed, washed thoroughly with deionized water to remove the solvent and impurities. After drying at 70 °C for 12 h in a vacuum oven, the chitosan/silk/zinc oxide composite was obtained.

Swelling studies

The kinetic swelling of the blends was measured in distilled water before and after zinc oxide mineralization. Swelling% during 24 h was calculated by the following equation:

$$\text{Swelling\%} = (\text{Wt} - \text{Wo})/\text{Wo} \times 100 \quad (1)$$

where Wo is the initial weight and Wt the final weight of the blends at time t.

Antibacterial test

The antibacterial activities of the chitosan/silk fibroin and chitosan/silk fibroin/zinc oxide nanocomposite were evaluated using the agar disk diffusion method against *Escherichia coli* (*E. coli*) and *Staphylococcus aureus* (*S. aureus*).³ The antibacterial activity was measured against 25 µL of aqueous dispersion solution. After 24 h of incubation at 37 °C, the diameters of the inhibition zones were measured at least three times and the results were given as average values.

Characterization

Attenuated total reflection-Fourier transform infrared spectroscopy (ATR-FTIR) was performed on a Thermo Nicolet FT-IR Nexus 470 with a diamond crystal. Scanning electron microscopy (SEM) was done on a Quanta 250 FEG (Field Emission Gun), provided with an EDX Unit (Energy Dispersive X-ray Analyses), with an accelerating voltage of 30 K.

Transmission electron microscopy (TEM) images were taken with a JEOL JEM-2100 electron microscopy at 100k× magnification, with an acceleration voltage of 120 kV. Contact angle measurements were performed on the samples (in the form of compressed discs) on a Digidrop GBX. In all the measurements, Milli-Q water was used.

RESULTS AND DISCUSSION

The current study investigates the capability of natural and sustainable polymers, such as chitosan and silk, to form homogenous and bioactive blends, followed by embedding zinc oxide nanoparticles. The conformation of the functional groups of chitosan, regenerated silk fibroin, chitosan/silk fibroin blend was investigated by FT-IR spectroscopy, as shown in Figure 1. The broad band around 3450 cm⁻¹ is attributed to -NH, -OH stretching vibrations of chitosan molecules. The weak band at 2921 cm⁻¹ is ascribed to -CH-stretch of chitosan. Moreover, chitosan exhibits

peaks at 1652 and 1535 cm^{-1} , which can be assigned to amide I and amide II, respectively. After blending with regenerated silk fibroin, the bands assigned to the peptide backbone of amide I (1624 cm^{-1}) and amide II (1525 cm^{-1}) absorptions were remarked, which may attributed to silk II structure.¹²

The prepared zinc oxide based nanocomposite was investigated using various polysaccharides as growth modifiers.^{26,27} The surface morphology of the regenerated chitosan/silk fibroin blend, before and after zinc oxide formation, was investigated using SEM. As can be seen in Figure 2, the surface morphology of the blend is relatively homogenous. Moreover, the silk-rich phase and

the chitosan-rich phase cannot be easily distinguished in this image. It can also be inferred that the chitosan interacts with the dissolved silk fibroin during blend formation and there is a good adhesion between the two phases. The formed zinc oxide layer shows the presence of microplates with $\sim 1 \mu\text{m}$ length. These plates consist of zinc oxide nanoparticles with the diameter of $\sim 50 \text{ nm}$, as shown in Figure 2C. Zinc oxide nanoparticles appear to be more distinct and uniform, likely due to the interaction between the chitosan/silk fibroin blend and the formed nanoparticles, which decreases the attractive forces among nanoparticles, reducing their aggregation tendency.

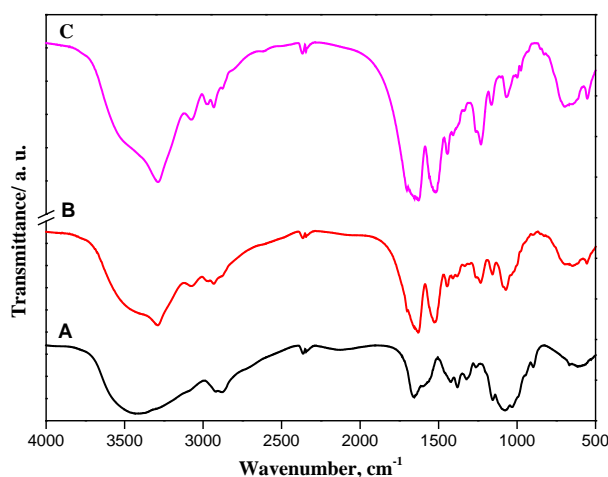


Figure 1: FTIR spectra of chitosan (A), silk fibroin (C) and chitosan/silk blends (B)

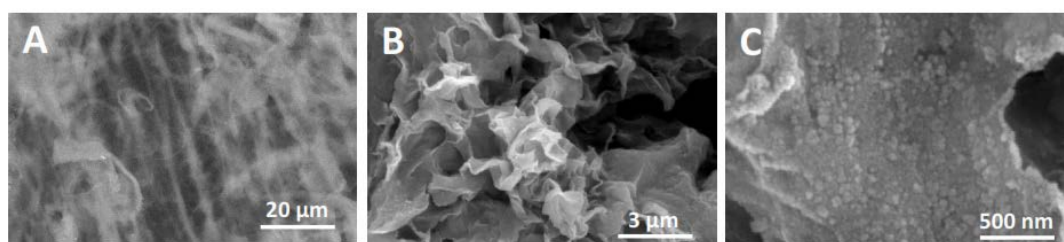


Figure 2: SEM of chitosan/silk fibroin blends before (A) and after (B and C) zinc oxide mineralization

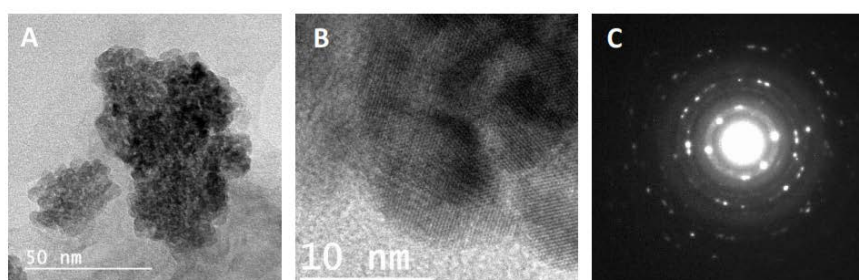


Figure 3: TEM image of chitosan/silk fibroin/zinc oxide hybrid

Direct proof of the formation of the chitosan/silk fibroin/zinc oxide nanocomposite is given by transmission electron microscopy (TEM), as shown in Figure 3. The nanocomposite is homogeneous and consists of densely packed nanospheres with a mean diameter of ~10 nm, which is smaller than that of the nanoparticles reported in the literature.^{26,28} High resolution transmission electron microscopy showed 2D lattice fringes of the nanocrystal particles with a distance ~0.25 nm between the adjacent lattice consistent with (100) reflection of zinc oxide nanoparticles. The selected area electron diffraction revealed the high crystallinity of the formed zinc oxide nanoparticles.

The polarity of the materials was determined by measuring the contact angle of the blend samples, as shown in Figure 4. Chitosan, a hydrophilic polymer, has amphiphilic character and a water contact angle of about $87^\circ \pm 4$. The contact angle decreased to $68^\circ \pm 3$ after blending

with silk fibroin, which may refer to an increase in hydrophilicity and wettability. The increasing hydrophilicity was expected to increase the contact between the blend surface and zinc oxide nanoparticles. Moreover, Figure 4 shows that the water contact angles of the chitosan/silk fibroin/zinc oxide hybrid film decreased from 68° to 45° , indicating that the surface of the chitosan/silk fibroin/zinc oxide nanocomposite is more hydrophilic. Moreover, the swelling% of the blends showed a significant increase from 107% to 131% after blending the chitosan with silk fibroin. However, there is no significant change in swelling% after zinc oxide mineralization, which supports the role of zinc oxide nanoparticles as crosslinking points between the polymer chains, preventing their expansion. This significant improvement in the hydrophilicity of the nanocomposite will be beneficial for cell adhesion, growth and wound healing applications.

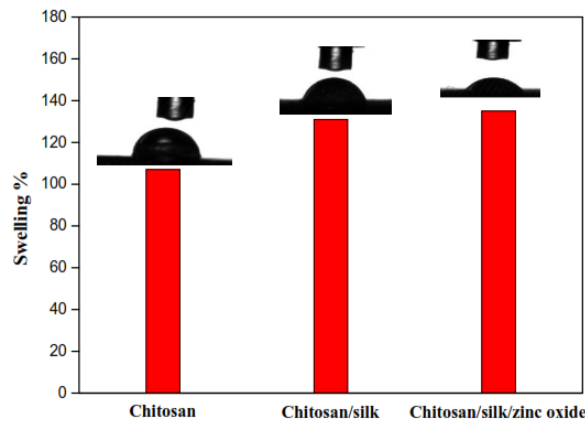


Figure 4: Swelling % and water contact angles of chitosan, chitosan/silk fibroin blend and chitosan/silk fibroin/zinc oxide nanocomposite

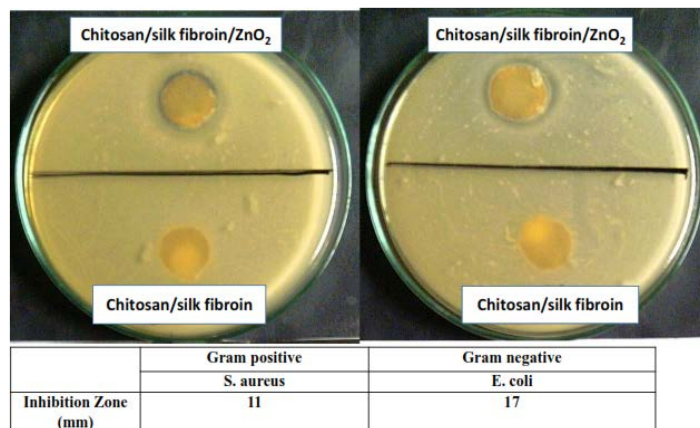


Figure 5: Representative photographs of the antimicrobial activity of chitosan/silk fibroin and chitosan/silk fibroin/zinc oxide nanocomposite against *Staphylococcus aureus* (left) and *Escherichia coli* (right)

Two strains, including a Gram-negative one (*E. coli*) and a Gram-positive one (*S. aureus*), were used for assessing the antimicrobial activity of the developed material. After calculating the antibacterial inhibition zone based on the disc diffusion method, the chitosan/silk fibroin blend was found not to exhibit any antimicrobial activity against Gram-negative or Gram-positive bacteria, as shown in Figure 5. However, the chitosan/silk fibroin/zinc oxide nanocomposite displayed an inhibition zone for both types of bacteria. The differences in the antimicrobial results may be due to the difference in the susceptibility of different bacteria to the prepared chitosan/silk fibroin/zinc oxide nanocomposite. The antibacterial mechanism of zinc oxide nanoparticles has not been completely understood yet. The most possible mechanism explains the antibacterial activity based on the zinc ions released from the zinc oxide nanoparticles, which strongly bind to the thiol groups on the cellular surface, leading to bacterial cell death.⁵ The present study indicates that the chitosan/silk fibroin/zinc oxide nanocomposite presents excellent antibacterial activity against both Gram-negative and Gram-positive organisms. The combination of all these beneficial qualities makes the prepared nanocomposite suitable for biomedical applications.

CONCLUSION

In summary, an environmentally friendly chitosan/silk fibroin/zinc oxide nanocomposite was prepared. Zinc oxide nanoparticles with uniform size were well dispersed on the surface of the chitosan/silk fibroin blend. The high crystallinity of the zinc oxide nanoparticles observed in this study suggested that natural polymers can serve as valuable mineralization additives for developing advanced nanocomposite materials. The prepared nanocomposite displayed highly effective antibacterial activity for different bacteria, which recommends the chitosan/silk fibroin/zinc oxide nanocomposite as a promising antibacterial agent for wound dressing.

ACKNOWLEDGEMENT: This work was supported by the National Research Center in Cairo, Egypt.

REFERENCES

¹ H. S. Hassan, M. F. Elkady, A. A. Farghali, A. M. Salem and A. I. A. El-Hamid, *J. Taiwan Inst. Chem. Eng.*, **78**, 307 (2017).

² M. S. Spencer, *Top. Catal.*, **8**, 259 (1999).

³ M. Ul-Islam, W. A. Khattak, M. W. Ullah, S. Khan and J. K. Park, *Cellulose*, **21**, 433 (2014).

⁴ R. R. Bacsa, J. Dexpert-Ghys, M. Verelst, A. Falqui, B. Machado *et al.*, *Adv. Funct. Mater.*, **19**, 875 (2009).

⁵ Y. W. Wang, A. Cao, Y. Jiang, X. Zhang, J. H. Liu *et al.*, *ACS Appl. Mater. Interfaces*, **6**, 2791 (2014).

⁶ D. R. Perinelli, L. Fagioli, R. Campana, J. K. W. Lam, W. Baffone *et al.*, *Eur. J. Pharm. Sci.*, **117**, 8 (2018).

⁷ A. Salama, R. E. Abou-Zeid, M. El-Sakhawy and A. El-Gendy, *Int. J. Biol. Macromol.*, **74**, 155 (2015).

⁸ A. Salama, *J. Colloid Interface Sci.*, **487**, 348 (2017).

⁹ S. Schweizer and A. Taubert, *Macromol. Biosci.*, **7**, 1085 (2007).

¹⁰ A. Salama, *Mater. Lett.*, **157**, 243 (2015).

¹¹ L. Al-Naamani, S. Dobretsov and J. Dutta, *J. Innov. Food Sci. Emerg. Technol.*, **38**, 231 (2016).

¹² J. Ming and B. Zuo, *J. Cryst. Growth*, **386**, 154 (2014).

¹³ Q. Yu, P. Wu, P. Xu, L. Li and T. Liu, *Green Chem.*, **10**, 1061 (2008).

¹⁴ S. Nardecchia, M. C. Gutiérrez, M. C. Serrano, M. Dentini, A. Barbeta *et al.*, *Langmuir*, **28**, 15937 (2012).

¹⁵ L. F. Zemljic and J. V. V. T. Kreze, *Cellulose Chem. Technol.*, **51**, 75 (2017).

¹⁶ X. Wang, J. Shi, Z. Li, S. Zhang, H. Wu *et al.*, *ACS Appl. Mater. Interfaces*, **6**, 14522 (2014).

¹⁷ M. D. A. Muhsin, G. George, K. Beagley, V. Ferro, C. Armitage *et al.*, *Biomacromolecules*, **15**, 3596 (2014).

¹⁸ A. Salama, *J. Carbohyd. Chem.*, **35**, 131 (2016).

¹⁹ M. B. Dickerson, S. P. Fillery, H. Koerner, K. M. Singh, K. Martinick *et al.*, *Biomacromolecules*, **14**, 3509 (2013).

²⁰ Y. Yang, H. Wang, F. Yan, Y. Qi, Y. Lai *et al.*, *Appl. Mater. Interfaces*, **7**, 5634 (2015).

²¹ L. Chen, J. Hu, J. Ran, X. Shen and H. Tong, *Int. J. Biol. Macromol.*, **65**, 1 (2014).

²² Y. Zhou, H. Yang, X. Liu, J. Mao, S. Gu *et al.*, *Int. J. Biol. Macromol.*, **53**, 88 (2013).

²³ X. Wang, T. Yucel, Q. Lu, X. Hu and D. L. Kaplan, *Biomaterials*, **31**, 1025 (2010).

²⁴ L. Liu, X. Zhang, X. Liu, J. Liu, G. Lu *et al.*, *ACS Appl. Mater. Interfaces*, **7**, 1735 (2015).

²⁵ X. N. Qi, Z. L. Mou, J. Zhang and Z. Q. Zhang, *J. Biomed. Mater. Res. - Part A*, **102**, 366 (2014).

²⁶ A. Khalid, R. Khan, M. Ul-Islam, T. Khan and F. Wahid, *Carbohyd. Polym.*, **164**, 214 (2017).

²⁷ R. Salehi, M. Arami and N. Mohammad, *Colloid. Surfaces B*, **80**, 86 (2010).

²⁸ S. K. Bajpai, M. Jadaun and S. Tiwari, *Carbohyd. Polym.*, **153**, 60 (2016).